Supporting Information

Flame Retardant Solid Polymer Electrolyte with Bridged Interface towards Safe and Stable Lithium-metal Batteries

Zhenxi Li,[a] Ruijie Guo,[a] Shilun Gao,[b] Yayue He,[c] Bing Yu,[d] Huabin Yang,*[ae] and Peng-Fei Cao*[d]

[a] Institute of New Energy Material Chemistry, School of Materials Science and Engineering, Nankai University, Tianjin 300350, China

[b] School of Integrated Circuit Science and Engineering, Tianjin University of Technology, Tianjin 300384, China

[c] Department of Materials Engineering, Taiyuan Institute of Technology, Shanxi, Taiyuan 030008, China

[d] State Key Laboratory of Organic-Inorganic Composites, School of Materials Science and Engineering, Beijing University of Chemical Technology, Beijing 100029, China

[e] Tianjin Key Laboratory of Metal and Molecular Based Material Chemistry, School of Materials Science and Engineering, Nankai University, Tianjin 300350, China

*Corresponding author: Huabin Yang and Peng-Fei Cao

Email address: hb_yang@nankai.edu.cn; caopf@buct.edu.cn

Experimental Section

Materials: Poly(ethylene glycol) methacrylate (PEGMA, average M_n = 500 g mol^{-1}), 3-(trimethoxysilyl)propyl methacrylate (MPS), hexamethylene Diisocyanate (HDI), triphenyl phosphate (TPP), 2,2'-Azobis(2-methylpropionitrile) (AIBN), Tetrahydrofuran (THF), SiO_2, and lithium bis(trifluoromethanesulfonyl)imide (LiTFSI) were purchased from Aladdin. All materials were used as purchased, without further purification.

Preparation of poly(PEGMA-*r*-MPS) and poly-PEGMA: PEGMA (4.5 g, 9 mmol), MPS (0.273 g, 1mmol), and AIBN (7.5 mg) were mixed in 40 ml THF and the solution was stirred at 70 °C for 24 h in a dry Ar atmosphere. The poly(PEGMA-*r*-MPS) was obtained after being dialyzed against the THF, followed by the rotary evaporation and vacuum-drying process. Following the same method, the poly-PEGMA was prepared without MPS monomer.

Preparation of cross-linked poly(PEGMA-*r*-MPS) and cross-linked poly-PEGMA: In the glovebox, the HDI and dibutyltin dilaurate were added to THF solution of poly(PEGMA-*r*-MPS) with the molar ratio of OH: NCO ~ 9:1, and the reaction was stirred at 70 °C for 6 h to obtain viscous cross-linked poly(PEGMA-*r*-MPS) solution. The cross-linked poly-PEGMA was prepared in the same method using HDI as the crosslinker.

Preparation of FRSPE-BI and FRSPE: The LiTFSI, SiO_2, and TPP were incorporated into the cross-linking poly(PEGMA-r-MPS) solution in a weight ratio of $m_{\text{cross-linked poly(PEGMA-r-MPS)}}$:$m_{\text{LiTFSI}}$: m_{SiO2}:m_{TPP} = 1:2:0.05:0.5 to produce the FRSPE-BI precursor solution. The resulting mixture was magnetic stirring for 6 h and ultrasonically agitated for 30 min to break the SiO_2 aggregated in a sealed container. The precursor solution for FRSPE was prepared by cross-linked poly-PEGMA, LiTFSI, SiO_2, and TPP in a weight ratio of 1:2:0.05:0.5. Then, the cellulose membranes were placed on Li metal anode, and the FRSPE-BI and FRSPE solutions were added to the membrane, respectively. Then, they were dried for 10 h at 65 °C to ensure complete evaporation of solvents to obtain the FRSPE-BI and FRSPE.

Material characterization: ^{1}H NMR spectra were recorded on a Bruker 400 MHz

NMR spectrometer using DMSO-d. Fourier transform infrared (FT-IR) spectra were recorded on a Nicolet iS50 FT-IR spectrometer (Bruker Tensor II) in the scanning range of 4000−400 cm^{-1}. The morphology of the electrodes was observed by a scanning electron microscope (SEM, JSM-7800F, JEOL, Japan). X-ray photoelectron spectroscopy (XPS) spectra were recorded from the Thermo Scientific ESCALAB 250Xi system. Before SEM and XPS characterizations, the samples were rinsed with pure DME or DMC solvent to remove the residual lithium salts and electrolyte and dried under a vacuum in the glovebox mentioned above. Then, they were transferred into these instruments with a special sealed device to avoid air exposure.

Battery assembly and measurement: For the cathode, $LiFePO_4$(LFP, HF-Kejing), Super P, and poly(vinylidene fluoride) binder (Kynar HSV900, ARKEMA) with the weight of 8:1:1 and then mixed with N-methylpyrrolidionon as the solvent. The slurry was first coated on an Al foil, which was then placed in a vacuum oven at 120 °C for 12 h. The mass loading of the LFP cathode was ~ 1-2 mg cm^{-2}.

The CR 2032-type coin cells were assembled in an Ar-filled glovebox with O_2 and H_2O contents below 1.0 ppm. The prepared FRSPE-BI was used as the electrolyte to the Li/FRSPE-BI/Li and Li/FRSPE-BI/LFP cells to evaluate the electrochemical performance.

The Li^+ transference number (strictly speaking, cationic transport number t_{Li^+}) was obtained via the potentiostatic polarization method in a symmetric Li/electrolyte film/Li cell according to the following equation:

$$t_{Li^+} = I_s(\Delta V - I_0R_0)/I_0(\Delta V - I_sR_s)$$

where I_0 and R_0 are the initial current and resistance, respectively, and I_s and R_s are the steady-state current and resistance after the polarization, respectively.

The ionic conductivity was obtained from the impedance measurements via the following equivalence

$$\sigma = l/RS$$

where l and S are the electrolyte film thickness (cm) and contact area (cm^2), respectively, and R is the ohmic resistance (Ω). R of electrolytes films was determined at room temperature by assembling electrolytes discs (Φ, ~16 mm) in 2032-type coin cells sandwiched between two steel spacers and using electrochemical impedance spectroscopy (EIS) on a Zennium Pro Electrochemical System in the frequency range of 1 MHz to 10 mHz with an amplitude of 5 mV.

The EIS test of Li/Li cells after cycling is measured at selected times under 0.1 mA cm^{-2} and 0.1 mAh cm^{-2}.

Density functional theory (DFT): The lowest unoccupied molecular orbital (LUMO) energy levels calculations were carried out by using the Gaussian 09 W program, and the molecular geometries for the ground states were optimized at the B3LYP/6-311G(d,p) level.[1]

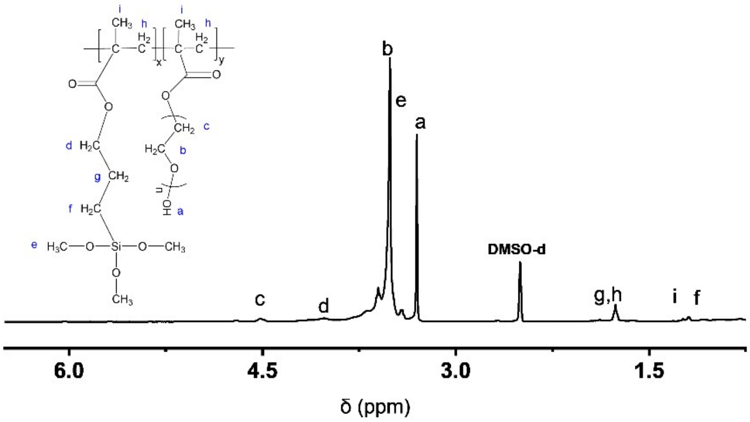

Fig. S1 ^{1}H NMR of the poly(PEGMA-*r*-MPS).

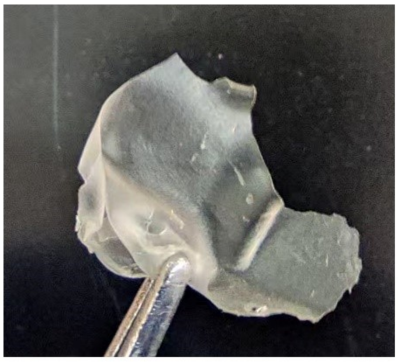

Fig. S2 The optical image of FRSPE-BI.

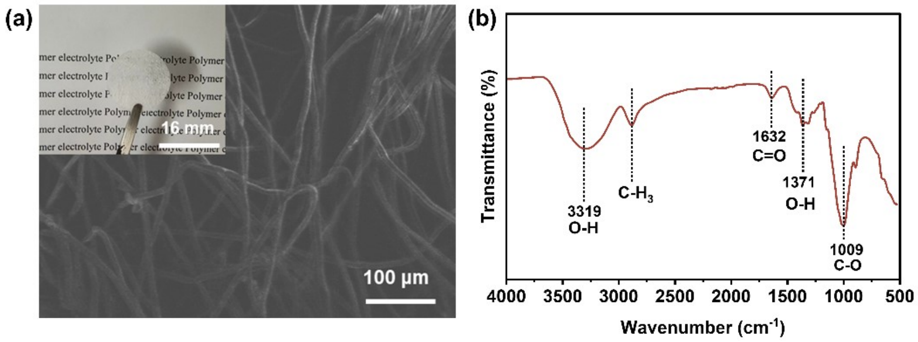

Fig. S3 (a) Digital photo and SEM image of cellulose fibers. (b) Total reflectance (ATR) spectrum of cellulose fibers.

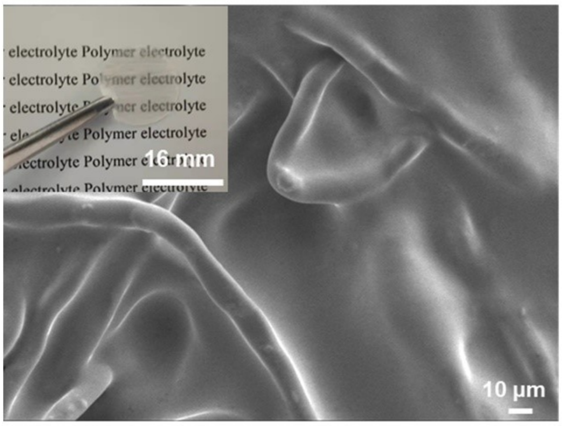

Fig. S4 The SEM images of FRSPE-BI membrane.

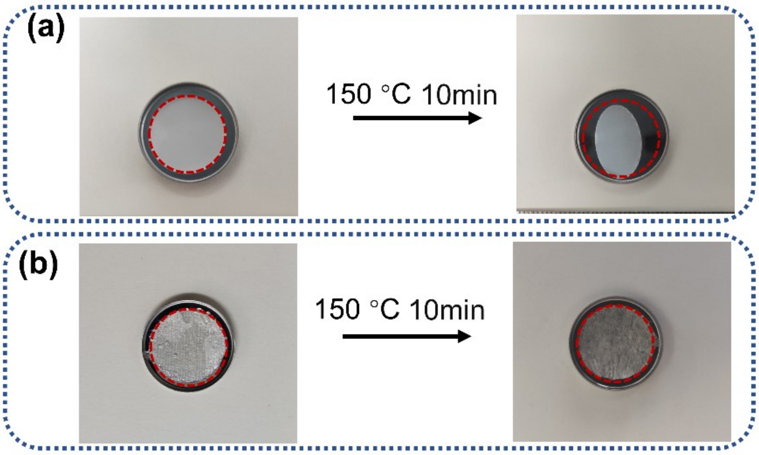

Fig. S5 thermal shrinkage of (a) PP separator and (b) FRSPE-BI membrane.

Fig. S6 Burning tests of SPE-BI membrane.

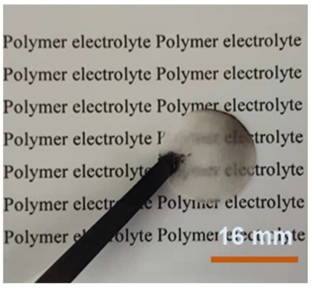

Fig. S7 Optical photos of FRSPE-BI membrane after three attempts to ignite.

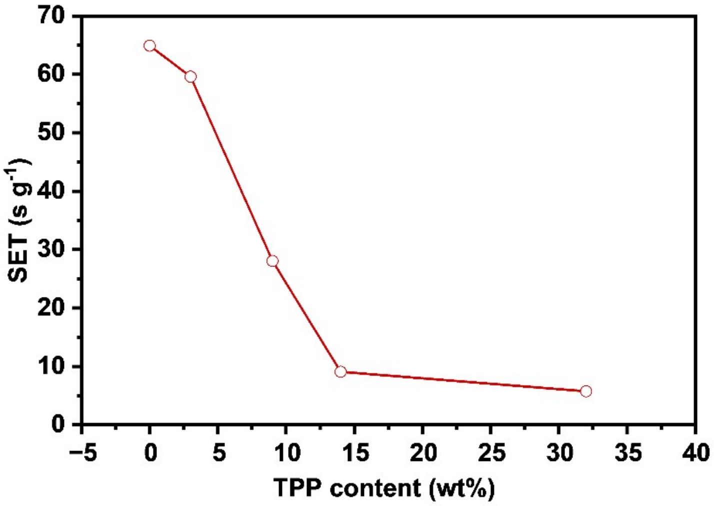

Fig. **S8** SET of the FRSPE-BI with different concentrations of TPP.

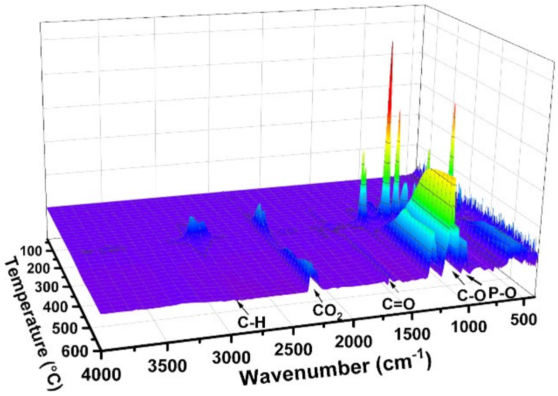

Fig. S9 3D TG-IR spectrum of the gases from thermal treatment of FRSPE-BI.

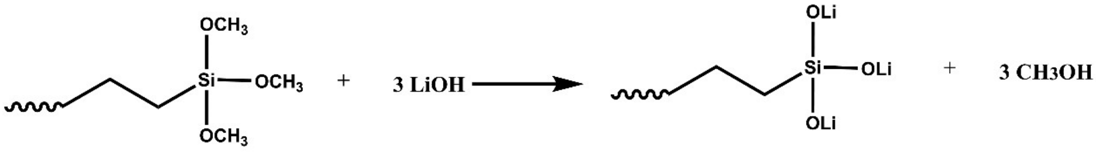

Fig. S10 The chemical reaction between MPS and Li anode.

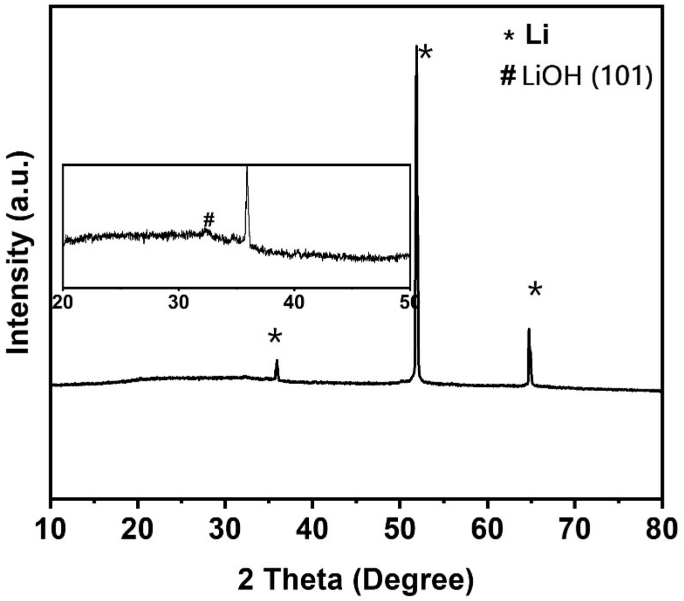

Fig. S11 XRD pattern of fresh pristine Li metal foil.

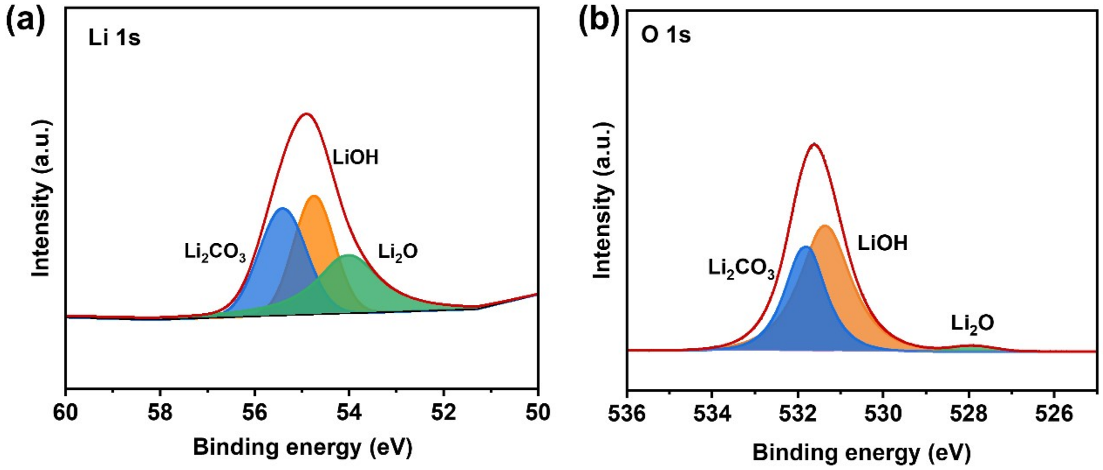

Fig. S12 XPS spectrum of (a) Li 1s and (b) O 1s for fresh pristine Li foils.

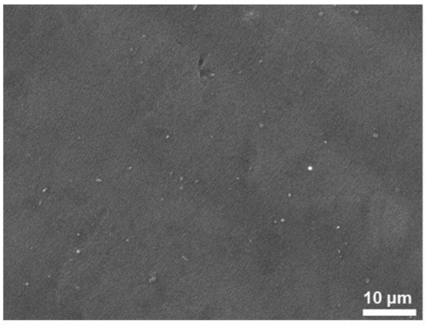

Fig. S13 Top-view SEM image of pristine Li.

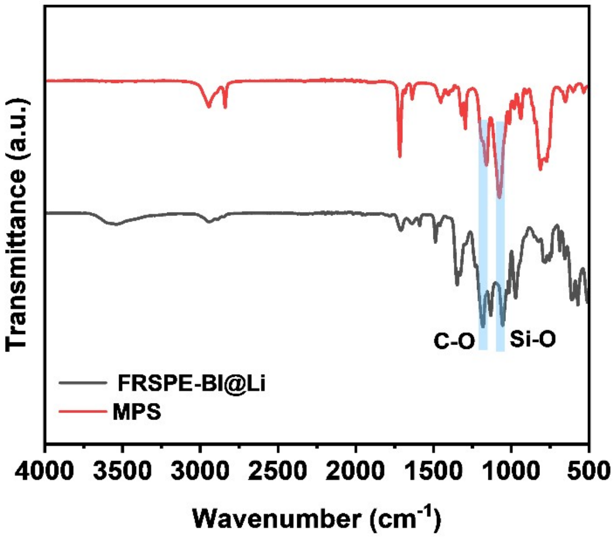

Fig. S14 the FT-IR spectra of FRSPE-BI and MPS.

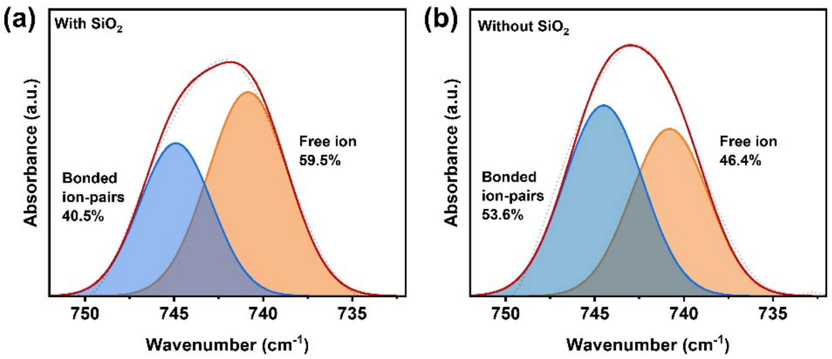

Fig. S15 FT-IR spectra of the FRSPE-BI with (a) and without (b) SiO_2 particles.

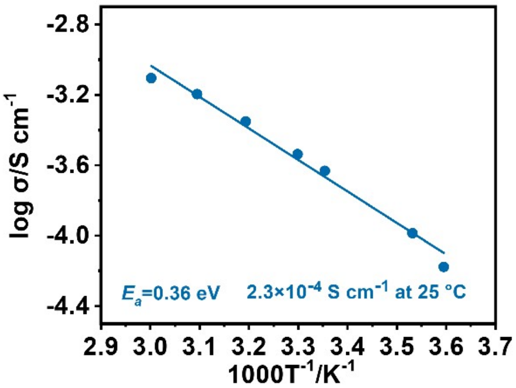

Fig. S16 FRSPE-BI without SiO_2 of ionic conductivities at different temperatures and fitted Arrhenius plots.

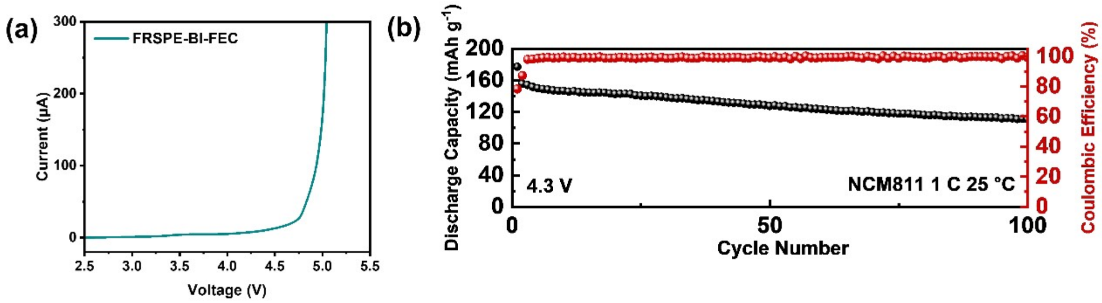

Fig. S17 The LSV curve of FRSPE-BI-FEC and cycle performance of Li/FRSPE-BI-FEC/NCM811.

Herein, we also introduced fluoroethylene carbonate (FEC, 5μL FEC was added to the side of the cathode) to improve the electrochemical stability window of such electrolyte system. The introduction of FEC improves the oxidation caused by the terminal -OH group in PEGMA when the voltage is higher than 4.05 V.[2, 3] With oxidation decomposition up to 4.3V (Fig. S17a), the FRSPE-BI (with additional FEC) based cell coupled with high voltage cathode $LiNi_{0.8}Co_{0.1}Mn_{0.1}O_2$ (NCM811) can also exhibit a good discharge capacity of 110.9 mAh g^{-1} over 100 cycles (Fig. S17b).

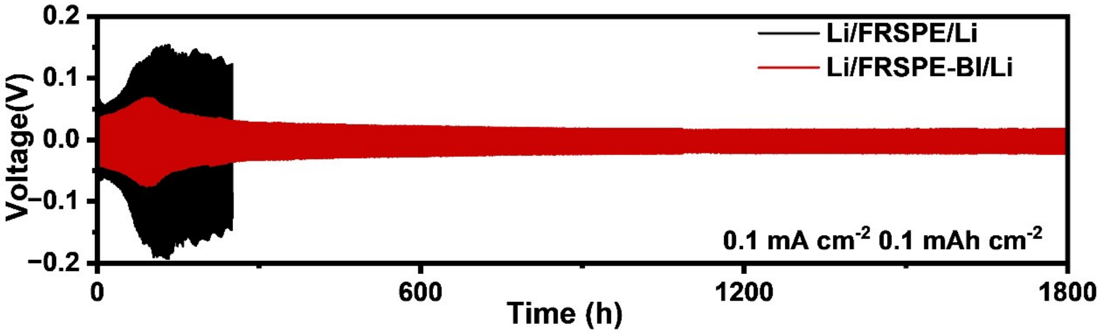

Fig. S18 The charge and discharge voltage profiles of Li/Li symmetric cells with FRSPE-BI and FRSPE at 0.1 mA cm^{-2} (capacity: 0.1 mAh cm^{-2}).

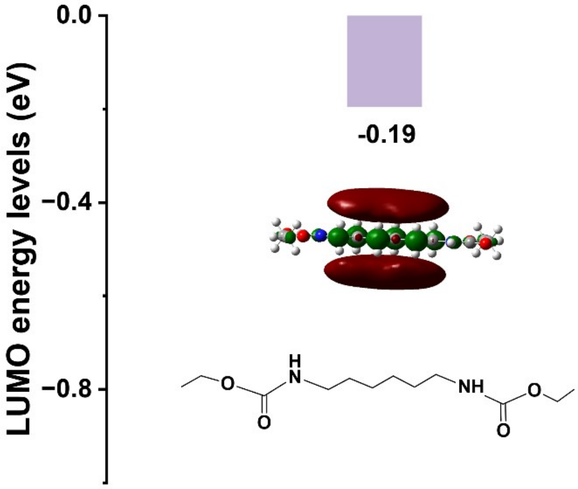

Fig. S19 The LUMO levels of crosslinker fragment.

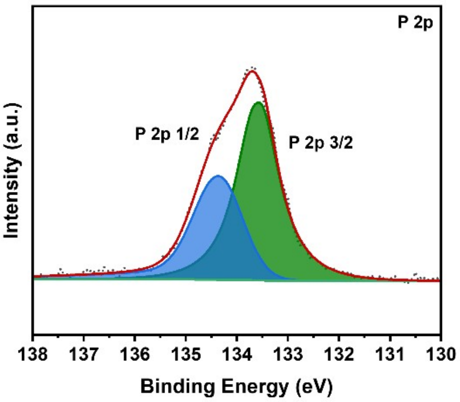

Fig. S20 XPS spectra of P 2p of Li metal from the Li/Li cells with FRSPE after 200 hours′ cycling at the current density of 0.2 mA cm^{-2}.

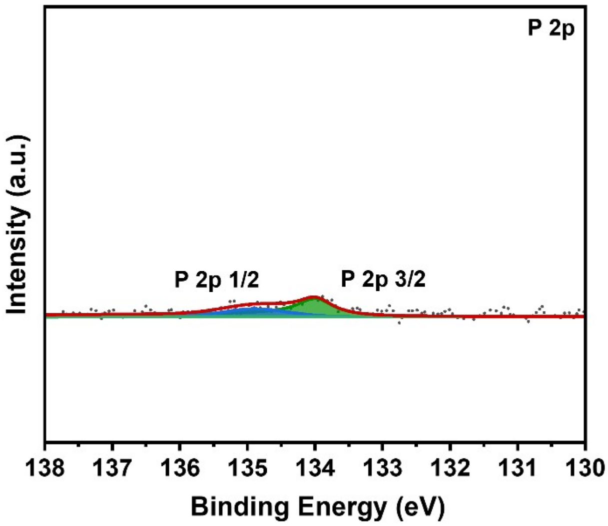

Fig. S21 XPS spectra of P 2p of Li metal from the Li/Li cells with FRSPE-BI after 200 hours′ cycling at the current density of 0.2 mA cm^{-2}.

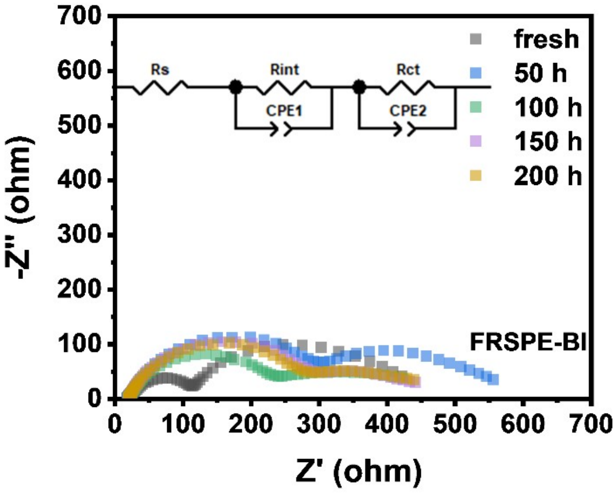

Fig. S22 The EIS of Li/Li cells using FRSPE-BI at different cycles.

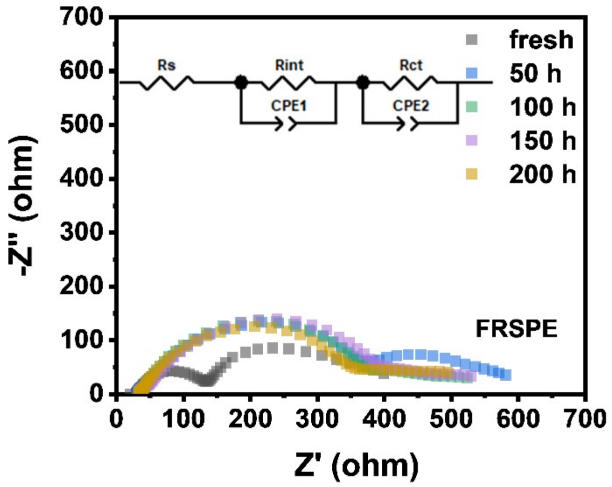

Fig. S23 The EIS of Li/Li cells using FRSPE at different cycles and equivalent circuit models.

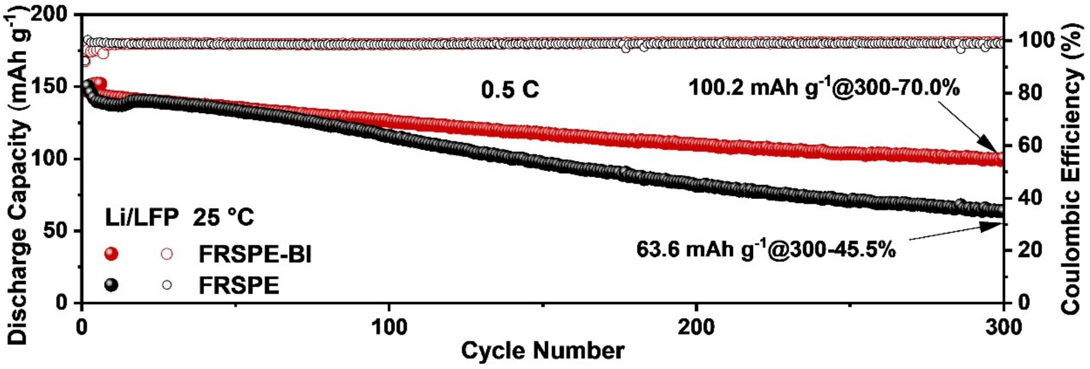

Fig. S24 Cycling performances of FRSPE-BI at 0.5C.

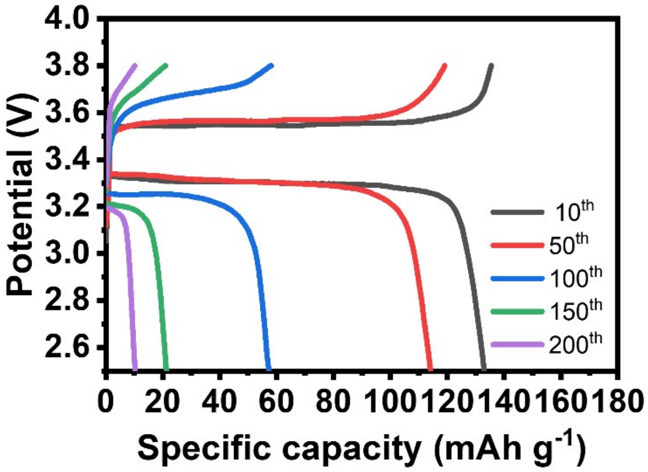

Fig. S25 Charge/discharge curves of the Li/LFP cell with FRSPE for the selected cycles.

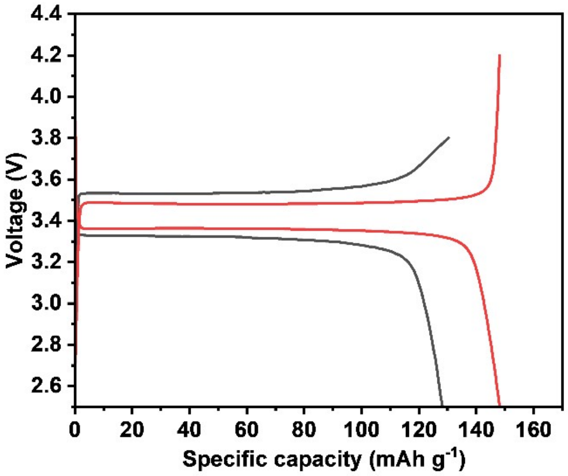

Fig. S26 Charge/discharge profiles of the cells with FRSPE-BI at 10th cycles in the potential range from 2.5-3.8 V and 2.5-4.2 V, respectively.

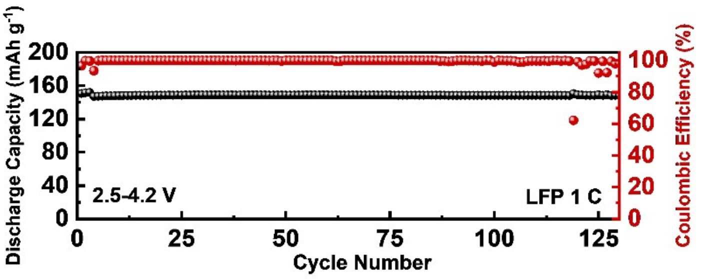

Fig. S27 The cycle performance of FRSPE-BI at 1 C and 4.2 V.

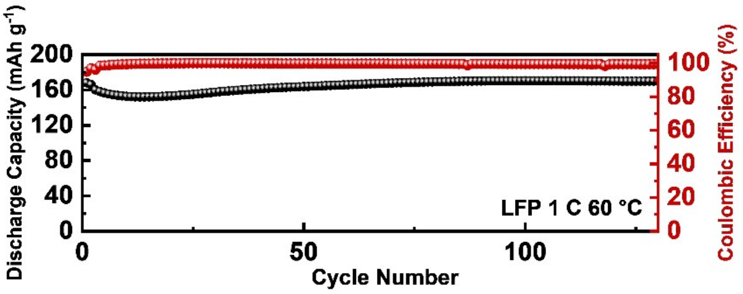

Fig. S28 Cycle performance of Li/FRSPE-BI/LFP cell at 1 C under 60 °C.

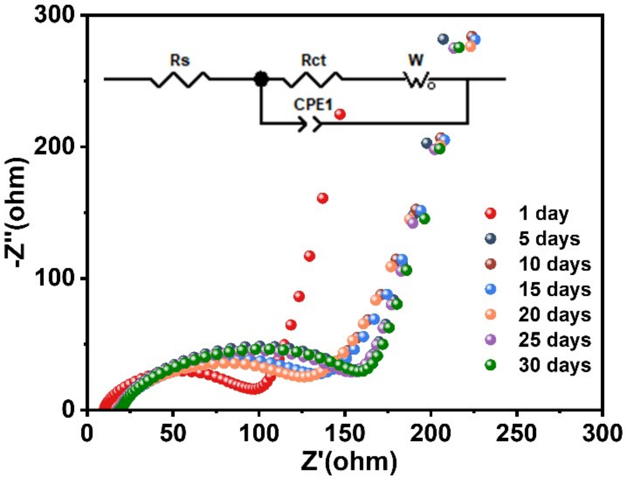

Fig. S29 EIS impedance spectra of Li/FRSPE-BI/LFP cell varying with the time at room temperature.

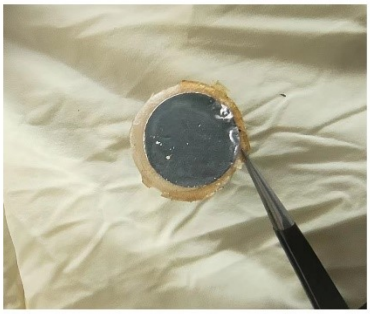

Fig. S30 Photographs of the good interfacial adhesion between FRSPE-BI and LFP cathode.

Table S1. Summary of flame retardant polymer electrolytes performance

No.	Electrolyte	Ionic conductivity (S cm^{-1})	t_{Li^+}	Full cell	Cycle performance Rate-life-capacity retention	Reference
1	FR-SPE1	7.08×10^{-5} (30 °C)	0.46	Li/LFP	0.2C-160 cycles	43
2	PVDF-LPPO	4.84×10^{-4} (25 °C)	0.47	Li/NCM	1C-1550 cycles-70.9%	44
3	P1-SPE	2×10^{-4} (70 °C)	0.26	Li/LFP	0.1C-100 cycles-66%	45
4	TH-PEO	4.5×10^{-6} (25 °C)	0.48	Li/NCM	0.5C-100 cycles-75.7%	46
5	PHPDEE-1:4	6.7×10^{-4} (RT)	0.31	Li/LFP Li/NCM	0.5C-550 cycles-99.1% 1C-500 cycles-70%	47
6	PHTY5	1.06×10^{-3} (RT)	0.41	Li/LFP	0.5C-500 cycles-98.14 %.	48
7	TESN	1.33×10^{-3}	0.48	Li/NCM-	0.5C-200 cycles-76.2%	49
8	**FRSPE-BI**	3.1×10^{-4} (25 °C)	**0.59**	Li/LFP	1C-300 cycles-76.7 %	**This work**

Reference：

1. V. A. Rassolov, M. A. Ratner, J. A. Pople, P. C. Redfern and L. A. Curtiss, *J. Comput. Chem.*, 2001, **22**, 976-984.
2. L. Seidl, R. Grissa, L. Zhang, S. Trabesinger and C. Battaglia, *Adv. Mater. Interfaces*, 2021, **9**, 2100704.
3. X. Yang, M. Jiang, X. Gao, D. Bao, Q. Sun, N. Holmes, H. Duan, S. Mukherjee, K. Adair, C. Zhao, J. Liang, W. Li, J. Li, Y. Liu, H. Huang, L. Zhang, S. Lu, Q. Lu, R. Li, C. V. Singh and X. Sun, *Energy Environ. Sci.*, 2020, **13**, 1318-1325.